Hydration and Mechanical Properties of Magnesia, Pulverized Fuel Ash, and Portland Cement Blends

L. J. Vandeperre[1]; M. Liska[2]; and A. Al-Tabbaa[3]

Abstract: A study was conducted to determine the quantity of water bound by hydration, the products formed during hydration, the microstructures, and the mechanical properties as a function of the relative content of reactive magnesium oxide (magnesia, MgO), pulverized fuel ash (pfa), portland cement (PC), and water used to prepare the mixes. It was confirmed that hydration of MgO leads to the formation of brucite and that PC forms its normal hydration products, even when both materials are present together. It was found that calculated changes in porosity and consumption of water during hydration based on the proposed hydration reactions agree well with the measurements. It was also found that the stiffness and strength improve directly proportional to the PC content. It is proposed that the lower strength of mixes with high reactive MgO contents is due to a combination of their high water demand and the difference in morphology between brucite and C–S–H gel.

DOI: 10.1061/(ASCE)0899-1561(2008)20:5(375)

CE Database subject headings: Construction materials; Portland cement; Fly ash; Admixtures; Mechanical properties; Compressive strength; Stiffness; Hydration; Microstructure.

Introduction

Production of portland cement (PC) causes significant CO_2 emissions. Part of the CO_2 emissions arise from the release of CO_2 from the conversion of the limestone used as a raw material, but also important is the fuel burned to heat the raw materials to 1450°C in the clinkering process. Given that the annual production of PC is about 2 billion t (Van Oss 2005), it is estimated that production of portland cement is responsible for about 10% of all CO_2 emissions due to human activity (Pearce 1997).

Not surprisingly there has been considerable effort to find alternatives for PC, and reactive magnesium oxide (MgO) cements were recently proposed as one such alternative (Harrison 2001, 2003). Reactive magnesium oxide cements are blends of a normal hydraulic cement, such as PC, reactive magnesium oxide, and often also a pozzolan such as pulverised fuel ash (pfa) or fly ash (Harrison 2001). Reactive MgO cements should not be confused with Sorel cements, which consist of magnesium oxychlorides or magnesium oxysulphates, or with magnesium phosphate cements. In reactive MgO cements, the contribution to setting by MgO is believed to be due to simple hydration to form magnesium hydroxide [brucite, $Mg(OH)_2$] (Harrison 2001). This hydration reaction has a particularly bad reputation among cement scientists as it is believed to give rise to unsoundness in portland cement (Hewlett 1998). However, hydration of MgO will only cause cracking when it occurs much later than the main hydration reactions and the hydration rate of MgO depends strongly on the calcination temperature (Hewlett 1998). Hence, MgO present as an impurity within PC is heated to 1450°C during clinkering, which leads to slow hydration and cracking. Reactive MgO, however, is calcined at much lower temperatures (<750 °C) (Harrison 2001) and retains a high surface area and porosity giving hydration rates not dissimilar to those of PC.

Although these reactive MgO cements have been known for about 5 years, there is still little quantitative data on the properties that can be achieved, especially for compositions containing substantial amounts of MgO. Therefore, in this paper experiments are reported which were aimed at: (1) determining the water to cement ratio which yields the highest strength and stiffness for reactive MgO cement blends of a wide range of compositions; (2) studying the hydration reactions to ascertain whether reactive MgO powders hydrate sufficiently rapidly, and to establish whether the hydration products are the same during simultaneous hydration of PC and MgO as when they hydrate separately; and (3) determining the major factors that influence the mechanical properties that are obtained.

Materials and Methods

The materials used in the blends were reactive magnesium oxide (MgO), pfa, and PC. To ensure that the results would not depend on a particular MgO source, two commercial reactive MgO powders were used (XLM, Causmag International, Young, Australia, and 05 CGU 98X, Unimag Ltd., Billingham, United Kingdom). The influence of the reactivity of the magnesium oxide powder was studied by also carrying out experiments with one dead

[1]Lecturer, Dept. of Materials, Imperial College London, Exhibition Rd., London SW7 2AZ, U.K.; formerly, Research Associate, Dept. of Engineering, Univ. of Cambridge, Cambridge CB2 1PZ, U.K. E-mail: l.vandeperre@imperial.ac.uk

[2]Ph.D. Student, Dept. of Engineering, Univ. of Cambridge, Trumpington St., Cambridge CB2 1PZ, U.K. E-mail: ml393@cam.ac.uk

[3]Reader in Geotechnical Engineering, Dept. of Engineering, Univ. of Cambridge, Trumpington St., Cambridge CB2 1PZ, U.K. (corresponding author). E-mail: aa22@cam.ac.uk

Note. Associate Editor: Chiara F. Ferraris. Discussion open until October 1, 2008. Separate discussions must be submitted for individual papers. To extend the closing date by one month, a written request must be filed with the ASCE Managing Editor. The manuscript for this paper was submitted for review and possible publication on January 9, 2007; approved on April 11, 2007. This paper is part of the ***Journal of Materials in Civil Engineering***, Vol. 20, No. 5, May 1, 2008. ©ASCE, ISSN 0899-1561/2008/5-375–383/$25.00.

Table 1. Chemical Composition and Physical Properties of Raw Materials

Compound or property	pfa		MgO			PC
	Rugby, classified	Ratcliffe, by-product	Causmag XLM	Unimag	DBM90	Lafarge blue circle
CaO	6.8	5.8	1.2	1.3	5.6	63.6
SiO_2	49.3	42.8	1.2	2.1	7.5	13.9
Fe_2O_3	9.7	10.4	0.2	0.8	0.9	2.7
Al_2O_3	24.1	29.2	0.2	(—)	3.4	10.2
MgO	1.1	1.3	97.2	95.8	82.6	0.6
K_2O	3.5	2.6	(—)	(—)	(—)	0.9
Na_2O	1.2	1.1	(—)	(—)	(—)	(—)
TiO_2	1.1	2.1	(—)	(—)	(—)	0.1
SO_3	3.3	4.0	(—)	(—)	(—)	6.9
Specific gravity	2.26	2.03	3.23	3.46	3.58	3.15
Mean diameter (μm)	12	56.5	31.1	10.7	35	(—)

burned magnesia (DBM 100) (Richard Baker Harrison, Ilford, United Kingdom). Dead burned MgO is nominally calcined at temperatures between 1500 and 2000°C. A pfa classified to conform to the British Standard for pfa for use in cement (BSI 1997) obtained from CEMEX United Kingdom, was used. A run of station pfa (E.ON, Ratcliffe-on-Soar, United Kingdom) was also examined to determine whether classification is really necessary to produce a useful addition to the MgO and PC blend. The same PC was used for all experiments (EN 197-1 CEM I, Blue Circle, Lafarge, United Kingdom). The density of the materials was measured by water displacement and the chemical composition of the materials was measured with an electron probe microanalysis system attached to a scanning electron microscope (SEM). The results are shown in Table 1 together with the mean particle size of the powders, measured by N. Vlasopoulos at Imperial College, London, using laser diffraction.

The blends of solids that were investigated included blends of MgO and pfa alone, blends of PC and pfa alone, and blends containing all three components at various levels, so that information on the hydration behavior of either MgO or PC could be contrasted with the behavior of combinations of PC and MgO. As the interest here is in cements with low embodied energy, all mixes contained a minimum of 50% by weight pfa. The effect of the type of MgO was studied by mixing each of the MgO powders with the same portland cement and the same pfa (Series A, B, and D in Table 2). The influence of the pfa source was studied by making a further set of mixes with the classified pfa and a single MgO powder (Series P in Table 2). For each of the solid compositions, the water content was varied so that the optimal water to solids ratios could be determined. The lowest and highest water contents were set to cover the entire range of types of pastes from crumbly powder mixes to slurries.

The blends were homogenized using a laboratory bench-top mixer. The density of the as-mixed pastes and slurries was measured. Samples were prepared by casting or placing into cylindrical molds ($\varnothing 50 \times 100$ mm). Care was taken to reduce the amount of air voids as much as was practically possible. For mixes with a paste-like consistency this required some compression to be exerted on the pastes, and at the lowest water contents of each series, compaction became increasingly difficult until finally full compaction could no longer be achieved. After 1–2 days of hydration under 98% relative humidity (RH), the samples were removed from the molds and left to hydrate further under the same conditions.

To study the hydration mechanisms, the crystalline phases that formed were determined by X-ray diffraction using Cu $K\alpha$ radiation (PW1050, Philips, Eindhoven, The Netherlands). Further, the quantity of water consumed during hydration was determined so that the stoichiometry of the hydration reactions could be confirmed. To determine the water consumed by hydration, the remaining quantity of evaporable water after an arbitrarily but fixed time period under saturated conditions (2 weeks, 98% RH) was determined by allowing the samples to dry out for 3 weeks in the ambient environment of the laboratory (30–45% RH) followed by drying crushed fragments even further by placing then in an oven at 105°C for 24 h. This procedure was used as it allowed differentiating to some extent between water in the larger pores, which will evaporate when exposed to ambient conditions, and water in the small pores, which due to capillary suction will not evaporate at the laboratory humidity level. In this paper, the total volume of water evaporated from the samples at 105°C will be referred to as the total porosity, whereas the volume of water evaporated in ambient conditions is taken as a measure of capillary porosity. This division is somewhat arbitrary and certainly qualitative as some structural water might have been lost from the C–S–H gel by drying at 105°C, but it was expected to be sufficiently indicative for establishing the trends in the behavior with varying composition.

The stiffness was characterized by determining the dynamic modulus from the resonance frequency (resonance frequency dynamic analyzer, IMCE, Diepenbeek, Belgium) (ASTM 2001). The unconfined compressive strength was measured according to BSI (2002) with the exception that the samples were not soaked prior to testing. The microstructure of the materials was studied by observing fracture surfaces of the broken samples in a SEM (JEOL 820, Japan).

Results

Water Consumption by Hydration

As shown in Fig. 1, the mass of most samples slightly increased by 1–2% during curing at 98% RH. This is not entirely surprising as the overall volume of the hydration products is often smaller than that of the water and the solids from which they form and since the volume of the samples remained constant within the accuracy of the measurement (±5%), this results in some space

J. Mater. Civ. Eng., 2008, 20(5): 375-383

Table 2. Composition of Mixes Investigated Expressed in Weight Fraction

		pfa		MgO			PC	
Code	Make up of mix	Rugby, BS	Ratcliffe	Causmag, XLM	Unimag 05 CGU 98X	Dead burned magnesia, DBM90	Lafarge, blue circle	w/s
P0	pfa_1	1.00		0.00			0.00	
P2	$(MgO_{0.8}PC_{0.2})_{0.1}-pfa_{0.9}$	0.90		0.08			0.02	0.275–0.45
P3	$(MgO_{0.5}PC_{0.5})_{0.1}-pfa_{0.9}$	0.90		0.05			0.05	0.25–0.65
P4	$PC_{0.1}-pfa_{0.9}$	0.90		0.00			0.10	0.25–0.50
P6	$(MgO_{0.8}PC_{0.2})_{0.5}-pfa_{0.5}$	0.50		0.40			0.10	0.30–0.60
P8	$PC_{0.5}-pfa_{0.5}$	0.50		0.00			0.50	0.20–0.40
A0	pfa_1		1.00	0.00			0.00	
A1	$MgO_{0.1}-pfa_{0.9}$		0.90	0.10			0.00	0.30–0.50
A2	$(MgO_{0.8}PC_{0.2})_{0.1}-pfa_{0.9}$		0.90	0.08			0.02	0.30–0.60
A3	$(MgO_{0.5}PC_{0.5})_{0.1}-pfa_{0.9}$		0.90	0.05			0.05	0.25–0.50
A4	$PC_{0.1}-pfa_{0.9}$		0.90	0.00			0.10	0.20–0.40
A5	$MgO_{0.5}-pfa_{0.5}$		0.50	0.50			0.00	0.40–0.70
A6	$(MgO_{0.8}PC_{0.2})_{0.5}-pfa_{0.5}$		0.50	0.40			0.10	0.40–0.60
A7	$(MgO_{0.5}PC_{0.5})_{0.5}-pfa_{0.5}$		0.50	0.25			0.25	0.35–0.70
A8	$PC_{0.5}-pfa_{0.5}$		0.50	0.00			0.50	0.25–0.60
B2	$(MgO_{0.8}PC_{0.2})_{0.1}-pfa_{0.9}$		0.90		0.08		0.02	0.20–0.50
B3	$(MgO_{0.5}PC_{0.5})_{0.1}-pfa_{0.9}$		0.90		0.05		0.05	0.20–0.50
B6	$(MgO_{0.8}PC_{0.2})_{0.5}-pfa_{0.5}$		0.50		0.40		0.10	0.40–0.60
B7	$(MgO_{0.5}PC_{0.5})_{0.5}-pfa_{0.5}$		0.50		0.25		0.25	0.30–0.60
D1	$MgO_{0.1}-pfa_{0.9}$		0.90			0.10	0.00	0.25–0.45
D5	$MgO_{0.5}-pfa_{0.5}$		0.50			0.50	0.00	0.20–0.40
D3	$(MgO_{0.5}PC_{0.5})_{0.1}-pfa_{0.9}$		0.90			0.05	0.05	0.25–0.45
D7	$(MgO_{0.5}PC_{0.5})_{0.5}-pfa_{0.5}$		0.50			0.25	0.25	0.25–0.45

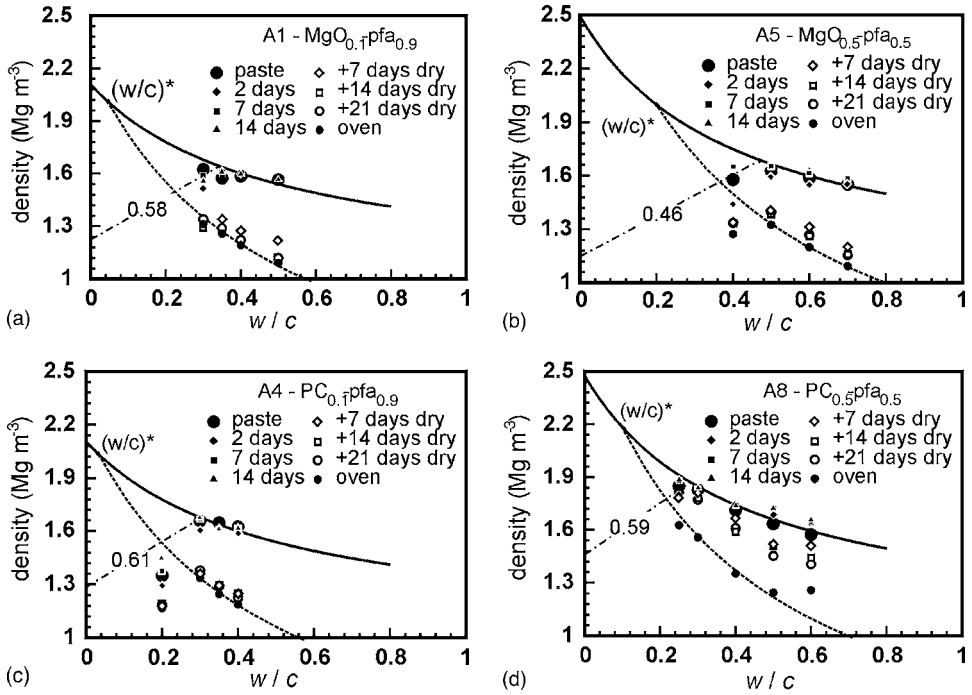

Fig. 1. Typical data of variation of density with water to solids ratio (w/s) at time of paste production, during curing in high humidity, and as drying proceeded

J. Mater. Civ. Eng., 2008, 20(5): 375-383

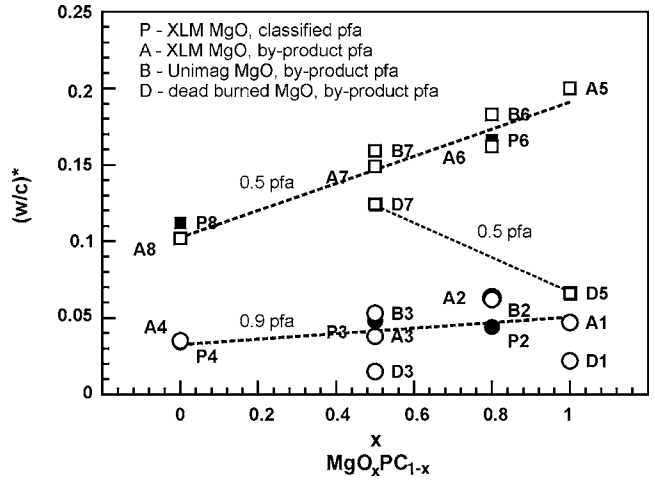

Fig. 2. Values of $(w/s)^*$ as function of relative quantity of MgO or PC in blend

becoming available for water uptake from the environment. Moreover, the presence of a small quantity of air within the samples is quite likely and these pores could slowly fill with moisture taken up from the saturated atmosphere.

As also shown in Fig. 1, the mass loss during drying occurs mostly while drying in ambient conditions. The mass loss during further drying at 105°C was highest in mixes with a high PC content as is clear from comparing Figs. 1(b and d). Assuming that initially the pastes are nearly air free, which is reasonable given the very small weight increase during curing under saturated humidity conditions, and assuming further that the water content of the mix does not influence the amount of water that is consumed by hydration per gram of solid $(w/s)^*$, the dry density is predicted to follow

$$\rho_{\text{dry}} = \frac{1 + \left(\frac{w}{s}\right)^*}{\frac{1}{\rho_s} + \frac{w}{s}} \tag{1}$$

where w/s=water to solids ratio by mass; and ρ_s=density of the mixture of solids. The dashed lines in Fig. 1 were obtained by fitting the dry density data to Eq. (1) to determine $(w/s)^*$. The good agreement confirms that the measured variation in dry density is consistent with the assumptions underlying Eq. (1). Large deviations did occur but only where the original density was much lower than what was predicted for a saturated paste (solid lines in Fig. 1)

$$\rho_p = \frac{s + w}{\frac{s}{\rho_s} + w} = \left(1 + \frac{w}{s}\right)\left(\frac{1}{\rho_s} + \frac{w}{s}\right)^{-1} \tag{2}$$

which, as discussed above, occurs when the water content is so low that the mixes cannot be compacted sufficiently to achieve the air-free density. For such samples Eq. (1) does not hold and therefore only points where the samples originally conformed to Eq. (2) were included in determining the water consumption by hydration $(w/s)^*$.

The quantity of water consumed per gram of solids is plotted as a function of composition in Fig. 2. For blends of PC, pfa, and reactive MgO (blends of Series A, B, and P), the quantity of water that has reacted with solids is found to vary linearly with composition. Moreover, from the positive slopes of the line, it is clear that the hydration of MgO consumes more water than the hydration of portland cement. When reactive MgO is replaced with a dead burned MgO (blends of Type D), this trend is reversed: the hydration of portland cement now consumes more water than the hydration of MgO, consistent with the expectation that the hydration of DBM is slow.

Table 3. Values of $(w/s)^*$ for Components in Mixes as Determined by Finding Least-Square Fit of Eq. (5) to Experimentally Determined $(w/s)^*$ for Mixes, Theoretical Estimate for $(w/s)^*$ for Full Hydration, and Estimated Amount of Water Needed Based on Amount of Unreacted MgO as Determined Using X-Ray Diffraction

	$(w/s)^*$ theory	$(w/s)^*$ water consumption	$(w/s)^*$ XRD
Reactive MgO:			
Causmag XLM	0.447	0.386	0.407
Unimag 05 CGU 98X	—	0.437	0.411
Dead burned MgO:			
DB 100	—	0.128	0.161
Pfa:			
Classified pfa (Rugby)	—	0.003	—
By-product pfa (Ratcliffe-on-Soar)	—	0.008	—
Portland cement:			
Blue circle PC, Lafarge	0.240[8]	0.207	—

The linear relation between the quantity of water that is consumed during hydration and composition suggests that there is no interaction between the different solids: each hydrating solid binds with a given quantity of water to form the hydration products, which it would also have formed in the absence of the other components. Hence, the total water consumption can be described by

$$\left(\frac{w}{s}\right)^* = \sum_i f_i \left(\frac{w}{s}\right)_i^* \tag{3}$$

where $(w/s)_i^*$=quantity of water consumed in the hydration of component i. Least square fitting of the total water consumed as a function of the composition was used to estimate the water consumption of each of the components. The results are given in Table 3 and show that hardly any water is consumed in the hydration of pfa, while the estimates for MgO are close to the expected value for

$$\text{MgO} + \text{H}_2\text{O} \rightarrow \text{Mg(OH)}_2 \tag{4}$$

which requires 0.447 g water per gram of MgO. The MgO from Unimag appears slightly more reactive than the MgO from Causmag, while the dead burned MgO is clearly less reactive, consistent with the differences in specific surface area, as detailed in Table 1. The value found for portland cement, 0.207 g per gram of cement, is also reasonable as full hydration of portland cement requires 0.24 g water per gram of cement, and full hydration of portland cement in 14 days is not expected (Mindess et al. 2003).

The lack of interaction between the components of the blend is somewhat contradictory to the expected role of pfa, which is a pozzolan and should therefore react with calcium hydroxide formed during hydration of the PC (Mindess et al. 2003)

J. Mater. Civ. Eng., 2008, 20(5): 375-383

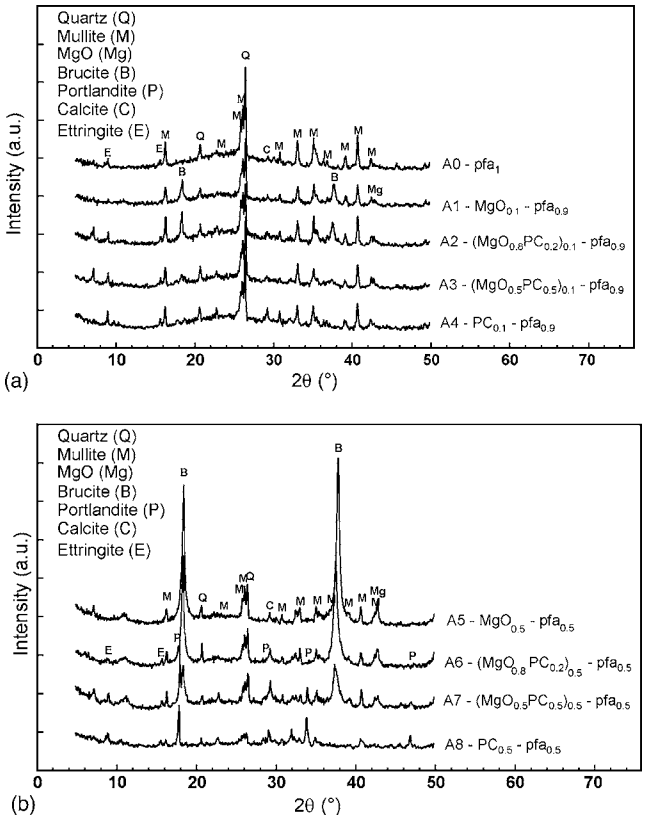

Fig. 3. X-ray diffraction patterns for samples made with pfa from Ratcliffe-on-Soar, Causmag XLM MgO powder, and PC: (a) mixtures of pfa alone or with weight fraction pfa of 0.9; (b) mixes with weight fraction pfa of 0.5

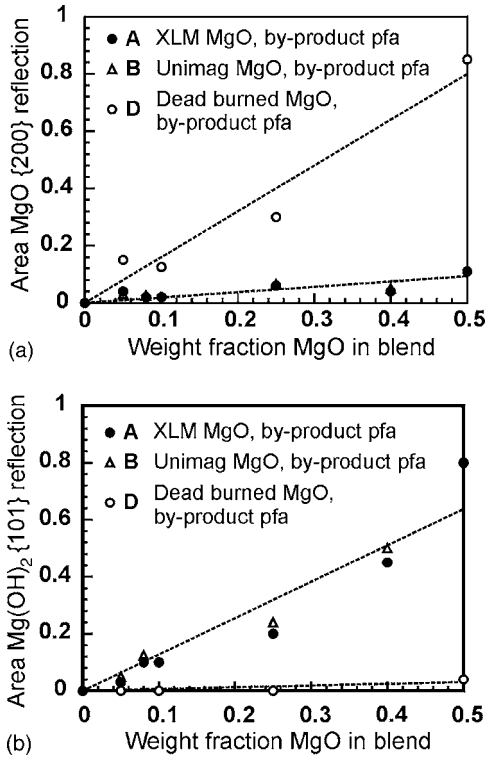

Fig. 4. (a) Area of {200} reflection of MgO in X-ray diffraction pattern as function of weight fraction MgO; (b) area of {101} reflection of brucite ($Mg(OH)_2$) in X-ray diffraction pattern as function of weight fraction MgO

$$3Ca(OH)_2 + 2SiO_2 + 5H_2O \rightarrow (CaO)_3 \cdot (SiO_2)_2 \cdot (H_2O)_8 \quad (5)$$

However, since the pozzolanic reaction can only occur when calcium hydroxide has formed first during the hydration of PC, its contribution to the overall water consumption will be proportional to the quantity of PC and therefore in the procedure used here it is included in the value attributed to PC. Moreover, pozzolanic reactions are slow (Wesche 1991) and will therefore only have occurred to a limited extent at the age of the samples studied here.

X-Ray Diffraction

Fig. 3 shows the X-ray diffraction (XRD) patterns collected for samples of Series A, produced using PC, the pfa from the Ratcliffe-on-Soar power station, and the Causmag XLM MgO powder. Although the pfa is to a large extent glassy, it also contains quartz and mullite, and peaks due to these materials therefore form an important part of all diffraction patterns obtained, consistent with what has been observed elsewhere (Wesche 1991). The pfa hydrates and carbonates to some extent even when it is used in isolation: ettringite and some calcite are present in samples containing only pfa (Type A0), whereas these phases are absent in the X-ray diffraction pattern of the raw material.

Further, the size of the strongest peak for MgO, marked Mg in Fig. 3, and of the peaks for brucite [$Mg(OH)_2$] increase with the quantity of MgO used in the blend. To show this clearer, the area of the {200} reflection of MgO ($2\theta = 42.87°$) and the area of the {101} reflection for $Mg(OH)_2$ ($2\theta = 37.38°$) are plotted against the weight fraction of MgO in Fig. 4. The linear relationship confirms that the degree of hydration of the MgO does not depend on the composition, and it is clear that when a dead burned MgO is used, instead of a reactive MgO, the quantity of residual MgO was much higher and the quantity of brucite formed much lower. The amount of unhydrated MgO was quantified by dividing the area of the {200} reflection of MgO by the area of the same peak in the diffraction pattern obtained for the MgO powder. The residual MgO content was 6.4 and 64% of the amount added for the reactive MgO powders and the dead burned MgO, respectively. As shown in Table 3, the amount of water needed to convert MgO into brucite calculated from the XRD estimate of the residual MgO agrees well with the direct measurements of the water consumption described above. This confirms that the approximate approach used to determine the water consumption gives reasonable results, at least as far as the hydration of MgO is concerned.

Hence, the major hydration reaction for MgO is clearly the formation of brucite. When no portland cement is added, the peaks for the brucite align better with the expected positions for these peaks, whereas when PC is present the {101} reflection is shifted toward lower 2θ values. This could indicate that some material is being incorporated into the brucite. The only other feature in the patterns that could indicate the presence of another crystalline hydration product is the low intensity and broad peak around $2\theta = 11°$, which is absent in the blends without MgO. It was not possible to attribute this peak to a known phase with a sufficient level of confidence, but one possible candidate is hydrotalcite [$Mg_6Al_2(CO_3)(OH)_{16}(H_2O)_4$], which is known to form during the hydration of mixtures of MgO and Al_2O_3 (Ahari et al. 2002).

The most important hydration product of portland cement, the C–S–H gel, is not crystalline and hence against the glassy back-

J. Mater. Civ. Eng., 2008, 20(5): 375-383

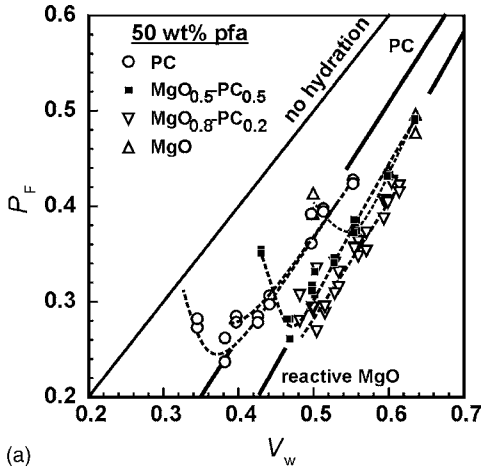

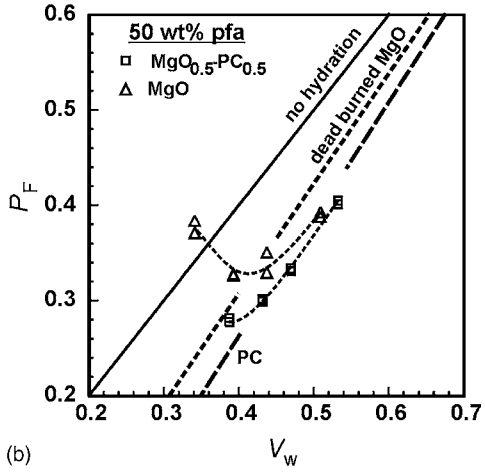

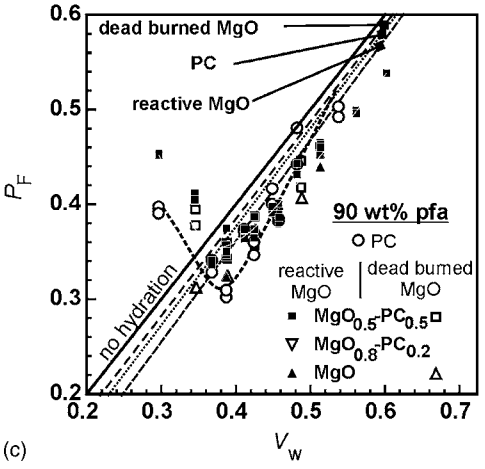

Fig. 5. Total porosity after hydration, P_F, versus initial volume fraction of water in paste mixes, V_w, for: (a) blends containing reactive MgO and 50% by weight pfa; (b) blends containing dead burned MgO and 50% by weight pfa; and (c) blends containing 90% by weight pfa

ground of the pfa it is impossible to detect its presence using X-ray diffraction. In fact, the same is true for M–S–H gels (Brew and Glasser 2005), which could have formed to some extent. However, typical crystalline hydration and carbonation products for portland cement such as ettringite, monosulfate, calcite, and portlandite were detected, suggesting that portland cement essentially hydrated as it would have done when no MgO was present. The water consumption attributed to PC, as shown in Table 3, is also largely consistent with this.

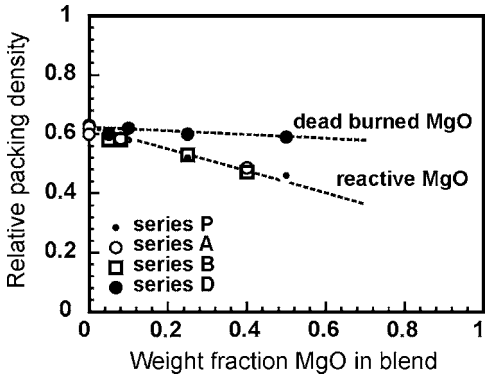

Fig. 6. Maximum packing density of solids in paste as function of solid weight fraction of MgO for range of combinations of powders

Microstructures

A wide range of water to solids ratios was used in the mixes tested and therefore, as shown in Fig. 5, porosity was found to vary accordingly. The results for the different series with reactive MgO (Series A, B, and P) were only marginally different and have therefore been taken together to make the plot clearer. As expected, the final porosity decreased as the quantity of water was reduced up until the point where compaction became difficult. Afterwards. lowering the water content led to higher final porosities. Hence, the minimum porosity versus water content can be considered as the optimal water content. Fig. 6 shows those optimal water contents, expressed as a packing fraction of the solids, for a range of compositions. The pfa, dead burned MgO, and portland cement can be used in widely varying ratios without affecting the ability to compact the mixes, giving packing densities of 0.56–0.6 consistent with typical values for portland cement (Kendall et al. 1983). Increasing the reactive MgO content, however, clearly reduced the best packing that could be achieved. Therefore increasing the reactive MgO content increased the lowest water content that should be used and hence also the porosity after hydration.

Fig. 5 also shows that for the same water content, the final porosity of the mixes of reactive MgO and pfa are lower than for similar mixes containing only PC and pfa, while the opposite is true when dead burned MgO was used. To quantify the expected pore volume fraction, a simple calculation was made, which accounts for the changes in volume that occurred during the hydration mechanisms proposed above. The porosity after hydration, P_F, is related to the initial volume fraction of water, V_w, by

$$P_F = (1 - \beta) + \beta V_w \tag{6}$$

where β = factor by which the solid volume increases upon hydration. For portland cement the solid volume of the hydration products was 503 mm^3 per gram of original cement (Mindess et al. 2003) or $\beta = 1.59$. Using the density of brucite (2.37 $Mg\,m^{-3}$) (Mindess et al. 2003) and the mass change upon the conversion of MgO into brucite of $Mg(OH)_2$, full hydration of 1 g MgO was found to yield 610 mm^3 brucite or $\beta = 2.18$. The lines added to Fig. 5 were calculated using Eq. (6) assuming the pfa is inert and using the degree of hydration for MgO as estimated from the

J. Mater. Civ. Eng., 2008, 20(5): 375-383

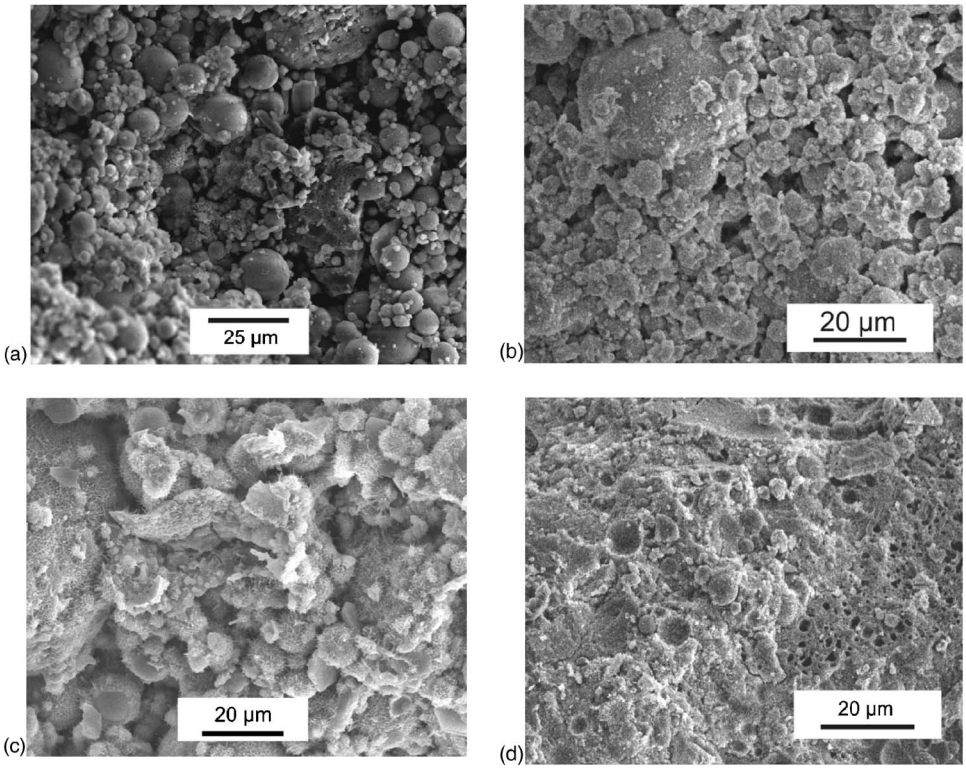

Fig. 7. Scanning electron micrographs of fracture surfaces of samples after 5 weeks (2 weeks of humid curing and 3 weeks of drying in ambient conditions). Samples shown are from Series A and had water contents close to optimal water content: (a) $MgO_{0.1}-pfa_{0.9}$, $w/s=0.35$; (b) $MgO_{0.5}-pfa_{0.5}$ $w/s=0.50$; (c) $PC_{0.1}-pfa_{0.9}$ $w/s=0.30$; and (d) $PC_{0.5}-pfa_{0.5}$ $w/s=0.25$.

X-ray diffraction results to account for the difference in reactivity of the two types of MgO. The predictions agree with the experimental trends reasonably well: the relative order reactive MgO, PC, and dead burned MgO is reproduced as is the effect of the pfa content on porosity.

Hence, the total porosity at the optimal water content is determined by two factors: the volume changes that occur upon hydration and the minimum water content that needs to be used to obtain a workable paste mix. Both can be illustrated with the actual microstructures of the materials. The effect of the volume changes is clear from the difference between the microstructures at optimal water content for mixtures with 90 or 50% by weight pfa [see Figs. 7(c and d)], while the higher porosity due to the higher water to solids ratios for high concentrations of MgO can be seen by comparing Figs. 7(b and d).

However, the observation of the microstructure of PC with 50% by weight pfa at w/c 0.25 as shown in Fig. 7(d) suggests that there was very little porosity while the measured total porosity at the same water content was substantial at 0.27 ± 0.2. This apparent difference can be understood by realizing that the measured total porosity was mainly gel porosity rather than capillary porosity. The observation that for a w/s of 0.25 hardly any water was removed by ambient drying as shown in Fig. 1(d) confirms this. In contrast, the total porosity for a mixture of reactive MgO with 50% by weight pfa for w/c 0.50 was measured at 0.38 ± 0.1, and although estimating pore volume fractions from fracture surfaces is difficult, the microstructure shown in Fig. 7(b) is clearly very porous. Moreover, as shown in Fig. 1(b), for this type of sample, almost all the water evaporated from the samples during ambient drying suggested that the porosity consisted of relatively large pores. The trend illustrated by these two examples is confirmed more generally when the ratio of capillary porosity over total porosity is plotted against composition as in Fig. 8, which shows that in addition to the expected increase in capillary porosity with an increase in water content, the capillary porosity also clearly decreased as the PC content was increased.

Hence, while it is true that more solid is formed during the hydration of 1 g MgO than of 1 g PC, MgO is less effective than PC at filling the free space and removing large pores because MgO forms a crystalline product, whereas PC forms a microporous gel.

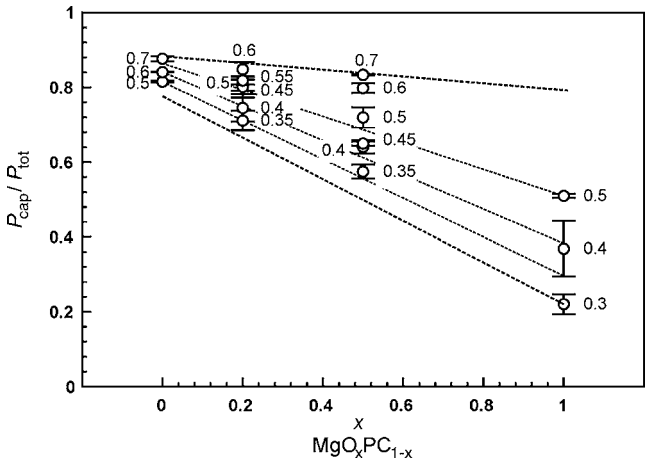

Fig. 8. Capillary porosity as fraction of total porosity versus composition for mixes with 50% by weight pfa. Data shown are average of all samples with reactive MgO (Series **A**, **B**, and **P**), which were compacted without difficulties.

J. Mater. Civ. Eng., 2008, 20(5): 375-383

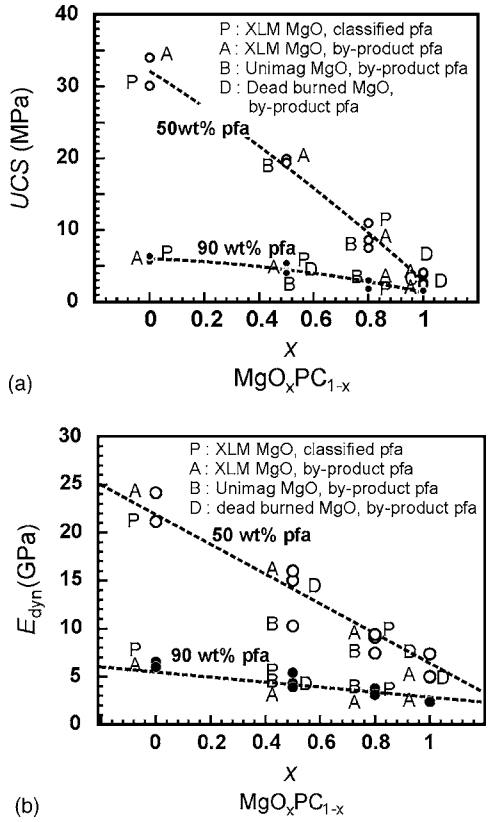

Fig. 9. Mechanical properties of mixes with w/c ratio giving lowest porosity as function of composition of mix in terms of: (a) unconfined compressive strength; (b) dynamic modulus

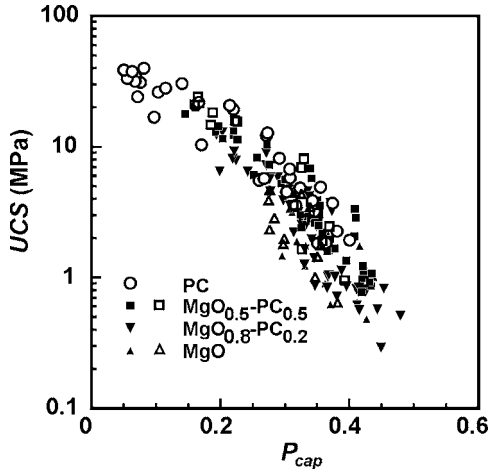

Fig. 10. UCS versus porosity for different mixes in which for mixes containing MgO open symbols represent mixes with dead burned MgO, while solid symbols represent mixes with reactive MgO

Mechanical Properties

Figs. 9(a and b) show the variation of the unconfined compressive strength (UCS), and dynamic modulus E_{dyn} with composition for mixes at the optimal w/s ratio defined above. Each data point shown is the average of 2–4 samples with a standard deviation of 5–10%. Comparing the two figures shows that strength and stiffness varied with composition in a very similar way. When a large fraction of the solids is pfa (90% by weight), there was only a small decrease in strength or modulus as PC was replaced by MgO and when less pfa was present (50% by weight pfa), there was a strong decrease in strength or modulus when PC was replaced by MgO.

As discussed above, the minimum porosity that can be achieved depended on the weight fraction MgO in the mix. Since in concrete and cement pastes, strength decreases rapidly as porosity increases, the observed trend versus composition might well be due entirely to the different minimum porosity levels that were achieved.

Further, it is well established that it is the capillary porosity rather than overall porosity, which is more detrimental to the strength (Kendall et al. 1983; Alford et al. 1985; Rößler and Odler 1985; Pettala 1992; Lokhorst and van Breugel 1997). Therefore, the variation in strength was plotted against capillary porosity in Fig. 10 in which each data point represents a single measurement. The fact that all the data line up into a single trend confirms that the major reason for the decrease in strength observed here was the capillary porosity. Hence, if reactive magnesia cements are to attain high compressive strengths, the water demand of the reactive powders must be addressed. However, the results also suggest that even if that is possible, the crystalline brucite formed during hydration of MgO will not be as effective as hydration of PC at eliminating the larger pores.

Conclusions

The quantity of water consumed by hydration was found to be linearly dependent on the composition of the blend, suggesting that there was no interaction between the components in the time scale of the experiments conducted here (14–35 days). The hydration of MgO and PC were found to consume 0.39–0.44 and 0.21 g of water per gram of solid, respectively, and the quantity of water consumed by direct hydration of pfa in the time frame was negligible. These values are in reasonable agreement with published values for PC and with the theoretical value for hydration of MgO assuming it forms brucite. X-ray diffraction confirmed that brucite was the main hydration product of MgO, and that all typical crystalline hydration products of PC were present when both PC and MgO were present together in the mix, confirming the assumption that both PC and MgO appear to hydrate independently of each other. It was established that as the quantity of reactive MgO was increased, the ability to obtain densely packed saturated and homogeneous paste mixes decreased, whereas pfa, dead burned MgO, and PC gave very similar best packing densities. Therefore, adding large quantities of reactive MgO while aiming for a workable paste led to microstructures, which were increasingly more porous before hydration began, and this offset the larger volume increase upon the hydration of MgO relative to PC so that the overall porosity after hydration increased with the reactive MgO content. Calculated total porosity after hydration using the assumed reactions gave good agreement with the observed changes in porosity. Furthermore, although the volume increase upon hydration was larger for MgO than for PC, in terms of reducing the capillary porosity PC was found to be more effective than MgO. The dynamic stiffness and unconfined compressive strength were found to depend directly on the volume fraction of the large pores present. Since saturated paste mixes containing reactive MgO remain more porous and contain a large fraction of large pores, the strength and stiffness were found to be reduced significantly when MgO replaced PC.

J. Mater. Civ. Eng., 2008, 20(5): 375-383

Acknowledgments

The work presented in this paper is the initial part of an extensive research programme being carried out as part of a U.K. Engineering and Physical Sciences Research Council (EPSRC) funding as a core Mini-Waste Faraday Partnership project entitled "Waste minimization through sustainable magnesium oxide cement products." The project is led by Cambridge University and carried out in collaboration with Imperial College London and MIT, United States, and ten industrial collaborators including the inventor of the MgO cement technology John Harrison of TecEco Pty Ltd., Australia. The financial support provided by EPSRC, under Grant No. GR/T26870/01, is gratefully acknowledged. The support from the Mini-Waste Faraday Partnership is also gratefully acknowledged. The writers are also grateful to Nikolaos Vlasopoulos at Imperial College for the measurements of specific surface area and particle sizes.

Notation

The following symbols are used in this paper:

P_f = porosity after hydration;
s = mass of solids;
V_W = initial volume fraction of water;
w = water of hydration;
w/s = water to solids ratio by mass;
$(w/s)^*$ = water consumed by hydration per gram of solid;
ρ_{dry} = dry density;
ρ_p = predicted density; and
ρ_s = density of solid mix.

References

Ahari, K. G., Sharp, J. H., and Lee, W. E. (2002). "Hydration of refractory oxides in castable bond systems. I: Alumina, magnesia, and alumina-magnesia mixtures." *J. Eur. Ceram. Soc.*, 22(4), 495–503.

Alford, N. M., Birchall, J. D., Howard, A. J., and Kendall, K. (1985). "Comments on 'The factors affecting strength of portland cement.' " *J. Mater. Sci.*, 20, 1134–1136.

ASTM. (2001). *Standard test method for dynamic Young's modulus, shear modulus, and Poisson's ratio for advanced ceramics by impulse excitation, ASTM C1259-01*, Philadelphia.

Brew, D. R. M., and Glasser, F. P. (2005). "Synthesis and characterisation of magnesium silicate hydrate gels." *Cem. Concr. Res.*, 35, 85–98.

British Standards Institution (BSI). (1997). "Part 1: Specification for pulverized-fuel ash for use with portland cement." *BS 3892*, London.

British Standards Institutions (BSI). (2002). "Testing hardened concrete. Part 3: Compressive strength of test specimens." *BS EN 12390*, London.

Harrison, J. (2001). *Reactive magnesium oxide cements*, WO 01/55049 A1.

Harrison, J. (2003). "New cements based on the addition of reactive magnesia to portland cement with or without added pozzolan." *Proc., CIA Conf.: Concrete in the Third Millennium*, CIA, Brisbane, Australia.

Hewlett, P. C. (1998). *Lea's chemistry of cement and concrete*, Arnold, London.

Kendall, K., Howard, A. J., Birchall, J. D., Pratt, P. L., Proctor, B. A., and Jefferis, S. A. (1983). "The relation between porosity, microstructure and strength, and the approach to advanced cement-based materials." *Philos. Trans. R. Soc. London, Ser. A*, 310(1511), 139–153.

Lokhorst, S. J., and van Breugel, K. (1997). "Simulation of the effect of geometrical changes of the microstructure on the deformational behaviour of hardening concrete." *Cem. Concr. Res.*, 27(10), 1465–1479.

Mindess, S., Young, J. F., and Darwin, D. (2003). *Concrete*, Prentice-Hall, Upper Saddle River, N.J.

Pearce, F. (1997). "The concrete jungle overheats." *New Sci.*, 155(2091), 14.

Pettala, V. E. (1992). "Nature of compression strength in concrete." *Mag. Concrete Res.*, 44(159), 87–106.

Rößler, M., and Odler, I. (1985). "Investigations on the relationship between porosity, structure and strength of hydrated portland cement pastes. I: Effect of porosity." *Cem. Concr. Res.*, 15(2), 320–330.

Van Oss, H., ed. (2005). "Mineral commodity summaries." *Survey USG*, 42–43.

Wesche, K. (1991). *Fly ash in concrete: Properties and performance*, Chapman and Hall, London.